Catalysis Today 150 (2010) 319–331

Contents lists available at ScienceDirect

Catalysis Today

journal homepage: www.elsevier.com/locate/cattod

Simulation of an industrial riser for catalytic cracking in the presence of coking using Single-Event MicroKinetics

R. Quintana-Solórzano [a,1], J.W. Thybaut [a,*], P. Galtier [b], G.B. Marin [a]

[a] Laboratory for Chemical Technology, Ghent University, Krijgslaan 281, S-5, B-9000 Ghent, Belgium
[b] Institut Français du Pétrole, Centre d'Etudes et de Développements, Solaize BP3, Autoroute A7-69, 69390 Vernaison, France

ARTICLE INFO

Article history:
Available online 2 September 2009

Keywords:
Catalytic cracking
Coke formation
Riser reactor
Single-Event MicroKinetics (SEMK)

ABSTRACT

A relumped Single-Event MicroKinetic model for the catalytic cracking of hydrocarbons and coke formation on a RE-USY equilibrium catalyst is used to simulate an industrial riser. In contrast to previous publications on the modeling of riser reactors for catalytic cracking, the current mode includes a fundamental description of the reaction pathway to catalytic coke, resulting in a slightly higher number of lumps, i.e., 677 + 1 for coke rather than 670. Coke formation occurs via alkylation of di and triaromatics, which are coke precursors formed during cracking or contained in the feed, with alkenes in LPG and gasoline fractions. A one-dimensional reactor model which is pseudo-homogeneous with respect to concentrations but heterogeneous with respect to temperature is used. Feed conversion as well as LPG, gasoline and coke yield profiles along the riser position are in line with published results showing a vigorous cracking and a moderate to fast coke deposition in the first meters. For a riser of 30 m length, about 70% of the cracked product yields and feed conversion is established during the first 3 m. The effect of operating conditions, feed composition and riser dimensions on the product distributions is assessed. The regenerated catalyst temperature and the catalyst to oil ratio are identified as the key operating parameters affecting the conversion and the cracked product distributions.

1. Introduction

The high economical benefits of Fluid Catalytic Cracking (FCC) make it an important process in a modern oil refinery [1]. It aims at producing lighter, more valuable, cracked products such as LPG, gasoline and middle distillates as well as light alkenes such as ethylene, propylene or isobutene from high molecular mass petroleum fractions, i.e., atmospheric and vacuum gas oils, residue fuels, etc. Currently, FCC is the major fuel, i.e., gasoline and diesel, manufacturing process [2]. The cracking takes place on a solid acid catalyst containing Y-zeolite as main active component at a relatively high temperature, i.e., around 800 K.

The yield of valuable cracked products depends on catalyst formulation, operating conditions and feed composition. The latter has been reported to determine about 80% of the behavior of a commercial FCC unit [3] and, hence, a kinetic model that allows describing coke formation using feed invariant parameters is of a great strategic importance. The thousands of compounds contained in an FCC feed can be classified into a limited number of hydrocarbon families, viz., alkanes, cycloalkanes and alkylaromatics. They react in a different manner owing to the different reaction families they can undergo resulting in a set of characteristic reaction products.

The commercial catalytic cracking catalyst, in particular the zeolitic component that provides most of the cracking activity, rapidly deactivates due to the inevitable deposition of heavy side products referred to as coke. The latter is inherently produced as a consequence of the formation of the desired hydrocarbon products with a larger hydrogen to carbon content compared to that of the feed. Coke deposition affects the cracking activity and selectivity along with the thermal balance of the FCC unit that, in principle, operates autothermally.

The complexity of the reaction pathway yielding coke greatly depends on the hydrocarbon nature. (poly)Aromatics, which have a basic character, and alkenes, that are rapidly protonated to produce carbenium ions, are known to exhibit a significantly higher coke selectivity compared with that of alkanes and cycloalkanes [4]. Even though coking is a complex process, there are only a limited number of elementary reactions families involved, i.e., hydride transfers, alkylations, cyclisations and deprotonations [5]. Cracking and coking occur in parallel and, hence, a kinetic model has to be constructed in such a way that

* Corresponding author. Tel.: +32 9 264 4516; fax: +32 9 264 4999.
E-mail address: Joris.Thybaut@UGent.be (J.W. Thybaut).
[1] Current address: Instituto Mexicano del Petróleo, Eje Central Lázaro Cárdenas 152, 07730 Mexico City, Mexico.

0920-5861/$ – see front matter © 2009 Elsevier B.V. All rights reserved.
doi:10.1016/j.cattod.2009.07.110

Nomenclature

a'	volumetric external surface area of the catalyst ($m^2\ m^{-3}$)
alk	alkylation
C_c	coke on catalyst ($kg_{coke}(kg_{cat})^{-1}$)
C_D	drag coefficient
C_c^o	coke content in the regenerated catalyst ($kg_{coke}(kg_{cat})^{-1}$)
c_p	molar heat capacity at constant pressure (J (mol K)$^{-1}$)
cycl	cyclisations
$D(m)$	desorption term that accounts for the fraction of product carbenium ions that desorbs via hydride transfer
d_p	catalyst particle diameter (m)
(de)alkyl	(de)alkylation reactions
dep	deprotonation
disp	disproportionation
endo-prsc	endocyclic protolytic scission
(exo)-prsc	(exocyclic) protolytic scission
g	gravitational acceleration (m s^{-2})
G_{cat}^o	catalyst mass flow rate at the riser inlet (kg s^{-1})
G_{gas}^o	gas oil mass flow rate at the riser inlet (kg s^{-1})
$G_{gas,i}$	outlet mass flow rate of the lump i in the gas phase (mol s^{-1})
$h_{gas\text{-}cat}$	solid–gas heat transfer coefficient (W (m^2 K)$^{-1}$)
htr	hydride transfer
$\tilde{k}$	single-event rate coefficient (kmol(kg_{cat}s)$^{-1}$ or kmol(kPa kg_{cat}s)$^{-1}$)
L_j	lump j
L_v	enthalpy of vaporization of the gas oil (J (kg)$^{-1}$)
LC	lumping coefficient
$Mw_{m,gas}$	average molecular mass of a mixture of main hydrocarbons (kg(mol)$^{-1}$)
m	carbenium ion type (secondary or tertiary)
n	carbenium ion type (secondary or tertiary)
nlump	number of lumps
n_e	number of single events
PCP-isom	isomerization involving protonated cyclopropane intermediates
p_i	partial pressure of species or lump i (kPa)
par	number of alkanes (paraffins)
prot	protonation
prsc	protolytic scission
r	reaction rate (mol (kg_{cat} s)$^{-1}$)
$(r_c^o)_{alk\_side}$	initial rate of coke formation via side chain alkylation (kg (kg_{cat}s)$^{-1}$)
R_c	net production rate of coke kg (kg_{cat} s)$^{-1}$
R_i	net production rate of species or lump i (mol (kg_{cat} s)$^{-1}$)
s	secondary carbenium ion
T	temperature (K)
t	tertiary carbenium ion
u_i	interstitial velocity (m s^{-1})
u_s	superficial velocity (m s^{-1})
u_t	terminal velocity (m s^{-1})
x_{HCO} or x_{LCO}	heavy or light cyclic oil conversion (%)
x_c	mass yield of coke (kg_{coke} (kg_{feed})$^{-1}$)
x_i	mass yield of lump i in the gas phase (kg_i (kg_{feed})$^{-1}$)
x_i^o	mass fraction of lump i in the feed (kg_i (kg_{feed})$^{-1}$)
y_{i,L_1}	mole fraction of species i in lump L_1 (mol(mol)$^{-1}$)
z	position (m)

Greek letters

α	deactivation constant
endo-β-scission	endocyclic cracking in beta position
(exo)-β-scission	(exocyclic) cracking in beta position
ΔH_f^o	standard heat of formation (J mol^{-1})
ε	bed void fraction
λ	thermal conductivity (W (m K)$^{-1}$)
μ	viscosity (kg (m s)$^{-1}$)
ρ	density (kg m^{-3})
θ_B^+	fraction of acid sites covered by carbenium ions
$\theta_{H^+}^+$	remaining (free) fraction of acid sites in the catalyst
$\theta_{R_1^+}^+$	fraction of acid sites covered by a R_1^+ carbenium ion
Φ	deactivation coefficients
Ω	reactor or riser cross-section (m^2)

both processes are simultaneously addressed to explicitly account for the interaction between cracking and coking reactions [6]. This is, in a later stage, complemented with the commonly used deactivation functions to take into account the decrease in available acid sites due to acid site coverage and pore blockage by coke. Coke composition, on the other hand, is reported to be a strong function of temperature. At commercial cracking conditions, i.e., a temperature above 783 K, catalytic coke has essentially a polyaromatic character regardless the feed composition and catalyst properties [4].

Simulation models with a different degree of complexity have been reported for industrial FCC risers [7–15]. The degree of complexity is determined by the detail accounted for in the kinetics and in the reactor hydrodynamics. Kinetic models vary from drastically lumped to microkinetic ones, while hydrodynamic models range from pseudo-homogeneous 1D models to advanced 3D three-phase models [7] including Computational Fluid Dynamics type of equations. A very rigorous model for the riser was published by Theologos et al. [8]. It consisted of a set of three-dimensional partial differential equations that describes the catalyst distribution and gas velocity, pressure, component concentrations and temperature in the riser. Later, Das et al. [9] also performed a three-dimensional simulation of a riser. Most of the riser simulations, however, are based on 1D [10–12] and 2D models [13–15]. In general, the most complete simulation models from the hydrodynamics point of view, rely on relatively simple kinetic models using drastic lumping, i.e., 4-lump, 6-lump and 12-lump models [8,9], which despite their simplicity have as a major disadvantage that the corresponding rate coefficients are feed dependent. The higher the number of lumps considered, i.e., the more sophisticated the kinetic model, the less complex the hydrodynamic model that is generally used. The current challenge is to combine complex kinetics with complete hydrodynamics.

The most salient feature of the riser simulations presented in this work lies in the kinetics domain where the Single-Event MicroKinetics are incorporated for both the main hydrocarbons and the coke formation. The main advantage of using SEMK, based on free carbenium ion chemistry occurring on the Brønsted acid sites of zeolitic catalysts, is that the rate coefficients are feed independent [16]. The latter is an important aspect taking into account that the feed composition for catalytic cracking units continuously varies. In this model, a fundamental description of

the reaction pathway to catalytic coke is included leading to a slightly higher number of lumps than previously used [5]. A similar methodology was applied by others [17]. In that work, however, some global reactions are still present in the model, e.g., aromatization, whereas some relevant elementary reactions, e.g., cyclisation of acyclic species and nucleus alkylation of (poly)aromatics are not considered. Besides, no explicit distinction is made between coke precursors and coke, cfr. infra.

2. Riser model

In the commercial FCC unit, the cracking reaction essentially occurs in the riser. Vaporized, heavy hydrocarbons crack when contacting the hot catalyst coming from the regenerator. The formation of lighter products is invariably accompanied by catalyst deactivation due to coke deposition. The present work focuses on the simulation of the riser for which the following assumptions for the reactor model were made:

i. The riser is modeled as a tubular one-dimensional reactor where both axial and radial effective diffusion are neglected, i.e., ideal plug flow is assumed for both gas and solid phase.
ii. Mass balances are written pseudo-homogeneously, while the energy balance explicitly distinguishes between the vapor and the solid phase. As a result, a distinction is made between the gas and solid phase temperature. No intraparticle gradients are considered.
iii. Instantaneous vaporization of the feed occurs at the bottom of the riser.
iv. Adiabatic reactor operation.
v. Ideal gas behavior.

Hydrocarbon feeds up to C_{40} including (iso)alkanes, (iso)alkenes, (poly)aromatics, (poly)aromatic alkenes, (poly)cycloalkanes, (poly)cycloalkenes, cycloalkadienes, cycloalkane-(poly)aromatics, (poly)aromatics can be handled [18]. A total of 677 hydrocarbon lumps, vide Table 1, is considered in the model, whereas coke is an additional and a single lump. The contribution of thermal cracking products as well as thermal coke, the latter formed during the milliseconds at the riser inlet where the hot catalyst contacts the fresh feed, is not accounted for [19]. Moreover, other types of coke different from catalytic coke are not incorporated in the model.

2.1. Feed composition

The SEMK model requires a detailed analysis of the feed according to the lumps defined in the kinetics. The feed composition has to be given in terms of the constituting lumps per carbon number, cfr. supra. This requires important analytical efforts due to the large number of compounds contained. The carbon atom distribution per hydrocarbon type of a partially hydrotreated vacuum gas oil (VGO) used as feed during the simulations is given in Fig. 1 [20]. The global composition of this feed is 26 wt% alkanes, 18 wt% aromatics and 56 wt% cycloalkanes, with an average molecular mass of 316 g mol^{-1}, a density of 853.2 kg m^{-3}, a mean average boiling point of 685 K and a carbon to hydrogen ratio of 6.18 kg(kg)$^{-1}$.

Table 1
Lumps per hydrocarbon family considered in the riser simulator program.

Hydrocarbon type	Number of lumps	Carbon number
(iso)Alkanes	79	C_1–C_{40}
(iso)Alkenes	78	C_2–C_{40}
(poly)Cycloalkanes	126	C_5–C_{40}
(poly)Aromatics	116	C_6–C_{40}
(poly)Aromatic alkenes	108	C_8–C_{40}
Cycloalkane-(poly)aromatics	18	C_9–C_{14}
(poly)Cycloalkenes	126	C_5–C_{40}
Cycloalkene-(poly)aromatics	18	C_9–C_{14}
Cycloalkadienes	8	C_5–C_{12}

Apart from a detailed, laborious analysis, alternative methods are currently being explored to reconstruct the required characterization of heavy cuts from partial analytical data and macroscopic analyses. Hudebine and Verstraete [21] have developed a method for the molecular reconstruction of a light cyclic oil (LCO) fraction showing promising results for heavier hydrocarbons fractions.

2.2. Model equations

2.2.1. Mass balances

The following set of ordinary differential equations has been derived to calculate concentration profiles of the lumps in the gas phase, x_i, along the riser position, z:

$$\frac{dx_i}{dz} = \frac{\Omega_r \rho_{cat}(1-\varepsilon) R_i Mw_i}{G^o_{gas}} \quad (1)$$

with as inlet condition:

at $z = 0$, $x_i = x_i^o$

The corresponding continuity equation that described the formation of catalytic coke along the riser position, z, is given by

$$\frac{dx_c}{dz} = \frac{\Omega_r \rho_{cat}(1-\varepsilon) R_c}{G^o_{gas}} \quad (2)$$

with as inlet condition:

at $z = 0$, $x_c = x_c^o$

To be consistent with the mass balance equations for the gas phase hydrocarbons, Eq. (2) is given in terms of yield even though coke is not in the gas phase but on the catalyst covering its surface. A more rigorous set of equations for describing coke formation, involving a fully heterogeneous reactor model and accounting for internal diffusion limitations is beyond the scope of the current work.

Gas oils fed to an FCC unit typically contain some residual Conradson Carbon which consists of refractory hydrocarbons that, in the present work, are assumed to be fully transformed into catalytic coke resulting in x_c^o being different from zero.

The void fraction in the riser, ε, varies along the reactor position mainly due to gas phase composition changes. In addition, ε depends on the slip velocity which is defined as the difference between the interstitial velocity of the solid and the gas, cfr. infra. The slip velocity is approximated as the terminal velocity of an individual catalyst particle in the gas reactant mixture. This terminal velocity, u_t, is a function of the particle (catalyst) and the gas density:

$$u_t = \sqrt{\frac{4 g d_p (\rho_{cat} - \rho_{gas})}{3 \rho_{gas} C_D}} \quad (3)$$

In Eq. (3), d_p represents the average particle diameter, ρ_{gas} is the density of the gas phase products, that is mainly influenced by the composition and the temperature, and C_D is the drag coefficient that depends on the Reynolds number. Also:

$$u_t = u_{i,gas} - u_{i,cat} \quad (4)$$

$u_{i,gas}$ and $u_{i,cat}$ are the interstitial velocity for the gas and the catalyst, are defined in terms of the superficial velocity of the gas

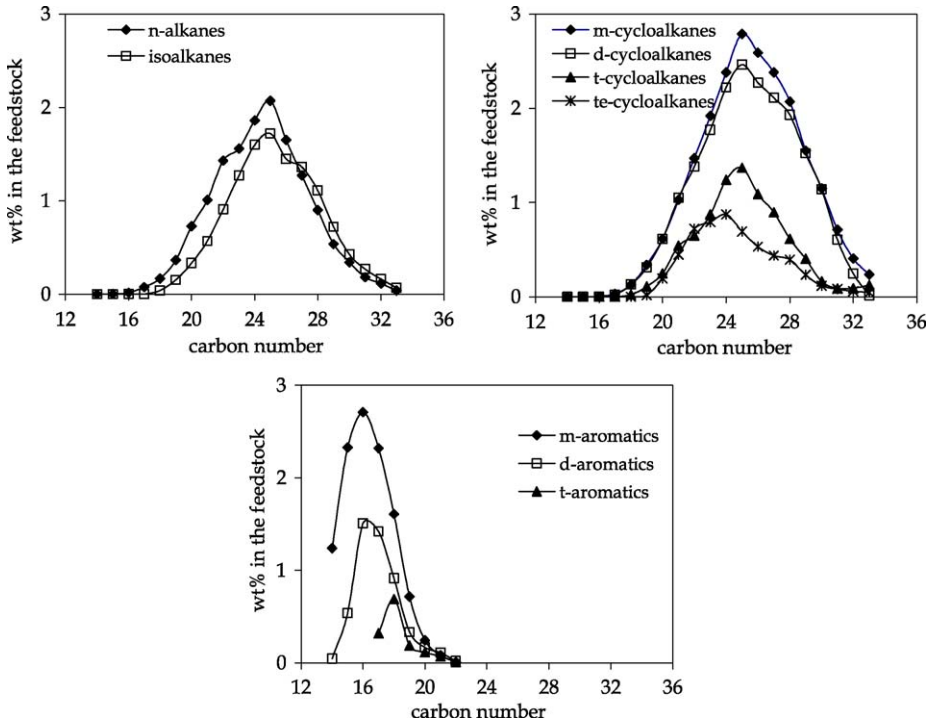

Fig. 1. Carbon atoms distribution per hydrocarbon family of the partially hydrotreated VGO used as feed in the simulations. M, d, t and te denote mono, di, tri and tetra ring structures.

and the solid, in the following way:

$$u_{i,\mathrm{gas}} = \frac{u_{s,\mathrm{gas}}}{\varepsilon} \tag{5}$$

$$u_{i,\mathrm{cat}} = \frac{u_{s,\mathrm{cat}}}{1-\varepsilon} \tag{6}$$

By substituting Eqs. (4) and (5) in Eq. (3), a quadratic expression for the void fraction, ε, is obtained:

$$\varepsilon(z) = \frac{(u_t + u_{s,\mathrm{gas}} + u_{s,\mathrm{cat}}) - \sqrt{(u_t + u_{s,\mathrm{gas}} + u_{s,\mathrm{cat}})^2 - 4u_{s,\mathrm{gas}}u_t}}{2u_t} \tag{7}$$

The superficial velocity of the solid and the gas, $u_{s,\mathrm{cat}}$ and $u_{s,\mathrm{gas}}$, respectively, are calculated by

$$u_{s,\mathrm{cat}} = \frac{G^{\mathrm{o}}_{\mathrm{cat}}}{\rho_{\mathrm{cat}}\Omega_r} \tag{8}$$

$$u_{s,\mathrm{gas}} = \frac{G^{\mathrm{o}}_{\mathrm{gas}}}{\rho_{\mathrm{gas}}\Omega_r} \tag{9}$$

$G^{\mathrm{o}}_{\mathrm{gas}}$ and $G^{\mathrm{o}}_{\mathrm{cat}}$ are the inlet mass flow rate of gas oil and catalyst. The gas density, ρ_{gas}, that depends on the gas phase composition and the temperature and on the total pressure is calculated using the ideal gas law. The catalyst density, ρ_{cat}, is assumed to be constant.

2.2.2. Energy balances

In the derivation of the energy balance, it is assumed that the feed instantaneously vaporizes at the riser inlet and, consequently, only a vapor and a solid phase are considered. The energy required for vaporizing the feed and for the endothermic cracking process is entirely supplied by the hot catalyst coming from the regenerator. In contrast to the mass balance, energy balance equations have been derived for the gas and the solid phase separately and, hence, the temperature gradient between solid phase, T_{cat}, and gas phase, T_{gas}, is explicitly accounted for. This is of particular importance at the riser inlet where catalyst and gas are not in thermal equilibrium. The dispersion steam that usually accompanies the feed during injection was not considered in the balance because it is typically added in low proportions, i.e., lower than 4 wt%.

The solid phase temperature is determined by the cracking reactions on the catalyst and by heat exchange with the gas phase. Accordingly, the catalyst temperature profile can be obtained from the following energy equation:

$$\frac{1}{\Omega_r} G^{\mathrm{o}}_{\mathrm{cat}} c_{p,\mathrm{cat}} \frac{\mathrm{d}T_{\mathrm{cat}}}{\mathrm{d}z} = (1-\varepsilon)[h_{\mathrm{gas-cat}} a'(T_{\mathrm{gas}} - T_{\mathrm{cat}}) - \rho_{\mathrm{cat}} \sum_{i}^{\mathrm{nlump}} \Delta H^{\mathrm{o}}_{f,i} R_i] \tag{10}$$

with the inlet condition:

at $z = 0$, $T_{\mathrm{cat}} = T_{\mathrm{cat,inlet}}$.

At the riser inlet, energy is transferred from the catalyst to the gas phase, while in the remaining part of the riser energy is supplied to the catalyst by the gas phase.

The gas phase temperature is only affected by energy transfer between the gas and the solid phase; consequently, the gas temperature profile can be determined from the following energy equation:

$$\frac{1}{\Omega_r} \sum_{i}^{\mathrm{nlump}} \frac{G_{\mathrm{gas},i} c_{p_i}}{Mw_i} \frac{\mathrm{d}T_{\mathrm{gas}}}{\mathrm{d}z} = (1-\varepsilon) h_{\mathrm{gas-cat}} a' (T_{\mathrm{cat}} - T_{\mathrm{gas}}) \tag{11}$$

with as inlet condition:

at $z = 0$, $T_{\mathrm{gas}} = T_{\mathrm{gas,preh}}$.

$T_{\mathrm{gas,preh}}$ corresponds to the gas oil preheating temperature and a' is the catalyst's volumetric external surface area, which for spherical particles corresponds to $6/d_p$; $h_{\mathrm{gas-cat}}$ is the gas–solid heat transfer coefficient, which was calculated via a semi-empirical equation reported by Han and Chung along the riser axis [22]:

$$h_{\mathrm{gas-cat}} = 0.03 \frac{\lambda_{\mathrm{gas}}}{d_p^{2/3}} \left[\frac{(u_{i,\mathrm{gas}} - u_{i,\mathrm{cat}})\rho_{\mathrm{gas}}\varepsilon}{\mu_{\mathrm{gas}}} \right]^{1/3} \tag{12}$$

μ_{gas} is the viscosity of the gas phase mixture which for simplicity was considered equal to 1.1×10^{-5} N s/m^2 independently of the position in the riser [15]. The thermal conductivity of the gaseous mixture, λ_{gas}, on the other hand, has also been computed using a correlation given by Han and Chung [22].

Notice that, in contrast to what is found in most of the literature dealing with riser simulations, the reaction enthalpy is not an average value but is calculated at different axial positions of the riser. This is important since it has been reported that the overall reaction enthalpy at the bottom of the riser can be more than three times higher than at the outlet [23] due to differences in gas phase composition and, hence, in cracking reactions that are taking place. The enthalpy of formation of a lump i at a given temperature, is calculated from its gas phase standard enthalpy of formation, $\Delta H^o_{f,i}$, and its gas phase molar heat capacity, c_{p_i}, as follows:

$$\Delta H^o_{f,i}(T_{gas}) = \Delta H^o_{f,i}(T_{ref}) + \int_{T^{ref}}^{T_{gas}} c_p \, dT \tag{13}$$

Both $\Delta H^o_{f,i}$ and c_{p_i} for a given lump are calculated via the group contribution method [24] at 298 K as reference temperature, T_{ref}.

The catalyst inlet temperature $T_{cat,inlet}$ used as inlet condition for Eq. (10) is obtained from the temperature of the regenerated catalyst, $T_{cat,reg}$, by accounting for the energy required for vaporizing the feed:

$$G^o_{cat} c_{p,cat}(T_{cat,reg} - T_{cat,inlet}) = G^o_{gas} L_v \tag{14}$$

The right hand side of Eq. (14) corresponds to the latent enthalpy required for the feed to be completely vaporized where L_v is the enthalpy of vaporization of the gas oil. Calculating a very precise value of L_v would require the heat of vaporization of all the hydrocarbons composing the feed, which is impractical. In our simulations a value of 180 kJ(kg)$^{-1}$ was utilized. This value lies in the range of heats of vaporization reported in the literature [8,11,25,26], i.e., 96 to 210 kJ(kg)$^{-1}$.

2.3. Numerical integration of the continuity equations

The number of ordinary differential equations to be integrated represented by Eqs. (1), (2), (10) and (11), amounts to 680, viz., 678 for the hydrocarbon lumps including coke, one for the catalyst temperature and one for the gas phase temperature. They were integrated simultaneously by using the LSODA subroutine [27]. This solver switches automatically between stiff and non-stiff methods. The simulations were performed on a PC equipped with a Pentium 4 processor. The calculation time depends on the step size chosen during the integration. Due to the high sensitivity of the rate coefficients to the temperature, a small size step was chosen to ensure smooth temperature variations, in particular, during the first centimeters of the riser. Using more than 2500 differential integration steps was found to be sufficient. The corresponding simulation took less than 3 min of CPU time.

3. Kinetics

In catalytic cracking, Single-Event MicroKinetics (SEMK) account for the detailed reaction network based on the classical carbenium ion chemistry occurring on the Brönsted acid sites of the catalyst. The carbenium ion stability is assumed to only depend on its type, i.e., primary, secondary or tertiary, determined by the number of alkyl substituents on the carbon atom bearing the charge. Excluding the unstable primary and methyl carbenium ions for most of the reactions from the considered network largely reduces the reaction possibilities and, consequently, the number of rate coefficients involved.

3.1. Relumped SEMK and corresponding rate equations

Due to the nature of feeds in catalytic cracking, SEMK have to deal with heavy hydrocarbons and complex mixtures of them. Despite the tremendous evolution of the available analytical techniques, a detailed analysis of complex mixtures along with the resulting cracked products is not fully feasible yet. Moreover, the number of species as well as the reaction possibilities grows exponentially with the carbon atom number. For a certain carbon number on, the reaction network becomes so overwhelming that working at molecular level becomes impractical and unnecessary. The integration of a large number of continuity equations for all the individual components in a reaction mixture would lead to excessive calculation times. Consequently, a certain degree of lumping is inevitable [18,28]. The relumping, as explained below, preserves the fundamental character of the model. The lumps' definition is inspired by the reaction products observed analytically, e.g., alkanes, alkenes, cycloalkanes, aromatics, etc., with a certain carbon number. Additionally, for alkanes and alkenes a distinction is made between linear and branched chains.

A typical relumping scheme illustrating the transformation via β-scission of alkanes contained in lump L_1 to alkenes in lump L_2 and alkanes in lump L_3 (or alkenes in lump L_4) is sketched in Fig. 2. First, alkanes contained in L_1 transform via hydride transfer to carbenium ions. β-Scission occurs on these carbenium ions to produce alkenes, lumped in L_2, and other carbenium ions. The latter can desorb through hydride transfer to a new lump of alkanes, L_3, or via deprotonation yielding a second lump of alkenes, L_4.

The lumped rate equation for a β-scission converting lump L_1 to lumps L_2 and L_3 corresponds to the summation of the reaction rates of the elementary reaction steps, which transform carbenium ions corresponding to the reactant lump L_1 to the alkenes in lump L_2 and the carbenium ions corresponding to the product lump L_3:

$$\begin{aligned} r_\beta(L_1 \rightarrow L_2 + L_3) = & \sum_{s,s} n_e \tilde{k}_\beta(s,s)\theta^+_{R_1(s)} D(s) \\ & + \sum_{s,t} n_e \tilde{k}_\beta(s,t)\theta^+_{R_1(s)} D(t) \\ & + \sum_{t,s} n_e \tilde{k}_\beta(t,s)\theta^+_{R_1(t)} D(s) \\ & + \sum_{t,t} n_e \tilde{k}_\beta(t,t)\theta^+_{R_1(t)} D(t) \end{aligned} \tag{15}$$

All possible carbenium ion types transformations, viz., (s,s), (s,t), (t,s) and (t,t), are taken into account. $\theta^+_{R_j^+(m)}$ denotes the fractional coverage of the Brønsted acid sites with the carbenium ion $R_1^+(m)$, cfr. infra, while $D(m)$ is a so-called desorption term that accounts for the fraction of product carbenium ions that desorbs via hydride transfer to alkanes in L_3:

$$D(m) = \frac{\tilde{k}_{htr}(m)\sum_{j=1}^{par}(n_e)_{htr} p_{P_j}}{(n_e)_{dep,av}\tilde{k}_{dep}(m) + \tilde{k}_{htr}(s)\sum_j (n_e)_{htr} p_{P_j} + \tilde{k}_{htr}(t)\sum_j (n_e)_{htr} p_{P_j}} \tag{16}$$

$\tilde{k}_{dep}(m)$ and $\tilde{k}_{htr}(m)$ are the single-event rate coefficients for deprotonation and hydride transfer, respectively, while $(n_e)_{av,dep}$ is the number of single events for a characteristic deprotonation.

In relumped form, Eq. (15) becomes:

$$\begin{aligned} r_\beta(L_1 \rightarrow L_2 + L_3) = & \tilde{k}_\beta(s,s) LC_\beta(s,s)\theta_{R_1^+(s)} D(s)\, p_{L_1} \\ & + \tilde{k}_\beta(s,t) LC_\beta(s,t)\theta_{R_1^+(s)} D(t)\, p_{L_1} \\ & + \tilde{k}_\beta(t,s) LC_\beta(t,s)\theta_{R_1^+(t)} D(s)\, p_{L_1} \\ & + \tilde{k}_\beta(t,t) LC_\beta(t,t)\theta_{R_1^+(t)} D(t)\, p_{L_1} \end{aligned} \tag{17}$$

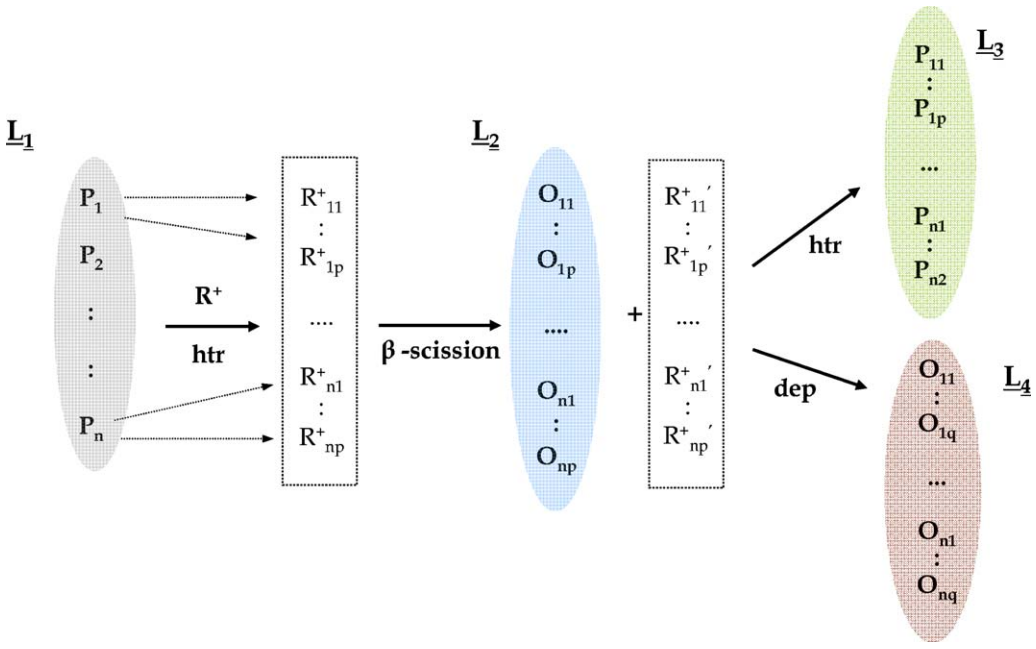

Fig. 2. Relumping scheme for the transformation of alkanes in lump L_1 to alkenes in lump L_2 and alkanes in lump L_3 (or alkenes in lump L_4) via β-scission.

The partial pressure of lump L_1, p_{L_1}, is incorporated into Eq. (17). The term $\theta^+_{R^+_i(m)}$ is calculated by assuming the pseudo-steady state approximation taking into consideration that carbenium ions undergoing β-scission can be formed out of alkanes in L_1 via hydride transfer, numerator, and can be consumed via deprotonation of hydride transfer, denominator:

$$\theta_{R_1^+}(m) = \frac{\theta_B^+ \tilde{k}_{\text{htf}}(m)}{(n_e)_{\text{dep,av}}\tilde{k}_{\text{dep}}(m) + \tilde{k}_{\text{htf}}(s)\sum_j (n_e)_{\text{htf}} p_{L_j} + \tilde{k}_{\text{htf}}(t)\sum_j (n_e)_{\text{htf}} p_{L_j}} \tag{18}$$

p_{L_j} is any hydrocarbon in the gas phase which can react via hydride transfer with the carbenium ions formed out of L_1 while θ_B^+ is the total surface coverage with carbenium ions. The latter is also calculated via the pseudo-steady state approximation by considering that carbenium ions are formed via protolytic scission, hydride transfer and protonation, and disappear via deprotonation and hydride transfer. The site balance on the catalysts is given by $1 = \theta_B^+ + \theta_H^+, \theta_H^+$ corresponding to the free sites.

$\text{LC}_\beta(m,n)$ in Eq. (17) are the so-called lumping coefficients that depend on the reaction network at elementary reaction level only, i.e., these coefficients are independent of the single-event rate coefficients and are calculated as follows:

$$\text{LC}_\beta(m,n) = \sum_{m,n}^{\text{par}} y_{i,L_1} (n_e)_\beta (n_e)_{\text{htr}} \tag{19}$$

For higher carbon numbers, i.e., exceeding 20, extrapolation formulas are used to calculate these lumping coefficients [18,29] because the reaction network generation for such high carbon numbers becomes impractical and unnecessary.

n_e is the number of single events for hydride transfer, responsible for the formation of secondary carbenium ions out of alkanes, and for the corresponding β-scissions. y_{i,L_1} denotes the molar fraction of the species i in the lump L_1, vide supra. For acyclic species, equilibrium composition within the lump is assumed while for cyclic ones an equimolar composition within the lump is used.

For the reactions involved in coke formation, relumping is also applied. Due to the intrinsic complexity of the coking process, the rate-determining step involved in coke formation is assumed to be nucleus and side chain alkylation of the corresponding (poly)aromatic coke precursors [5,30]. For instance, the relumped SEMK rate equation for coke formation through side chain alkylation of a lump L_1 containing triaromatics with the alkenes in lump L_2 is given by

$$r_c(L_1 + L_2 \rightarrow \text{coke}) = \tilde{k}_{\text{alk\_side}}(s,m) Mw_{\text{coke}} LC_{\text{alk\_side}}(s,m) \theta_{R_1^+(s)} p_{L_2} + \tilde{k}_{\text{alk\_side}}(t,m) Mw_{\text{coke}} LC_{\text{alk\_side}}(t,m) \theta_{R_1^+(t)} p_{L_2} \tag{20}$$

Triaromatic carbenium ions corresponding to the triaromatic components from lump L_1 are formed via hydride transfer. Note that, in contrast to Eq. (18), Eq. (20) does not contain any desorption term taken into consideration that coke is irreversibly adsorbed.

$\theta_{R_1^+(m)}$, the fractional catalyst surface concentration of secondary or tertiary carbenium ions formed out of lump L_1 via hydride transfer is calculated by assuming the pseudo-steady state approximation as has been explained above, vide Eq. (18). In Eq. (20), $\tilde{k}_{\text{alk\_side}}$ is the single-event rate coefficient for the side chain alkylation involved in coke formation, Mw_{coke} is the average molecular mass of coke and $\text{LC}_{\text{alk\_side}}$ is the lumping coefficient for the corresponding alkylation. The latter is calculated as follows:

$$\text{LC}_{\text{alk\_side}}(m) = \sum_m (n_e)_{\text{alk\_side}} (n_e)_{\text{prot}} y_{i,L_1} y_{j,L_2} \tag{21}$$

$(n_e)_{\text{alk\_side}}$ is the number of single events for the side chain alkylation while y_{i,L_1} represents the molar fraction of the triaromatic i in the lump L_1 and y_{j,L_2} the molar fraction of the alkene j in the lump L_2. Since alkylation is a bimolecular reaction, two mole fractions are needed to be included in Eq. (21), contrary to Eq. (19).

3.2. Reaction network

Table 2 presents a summary of the number of reactions, i.e., β-scissions, protolytic scissions, isomerizations, cyclisations, etc., occurring during the transformation of the different lumps of

Table 2
Summary of reactions for the relumped SEMK model involved in the cracking of the various lumps of hydrocarbons taken into consideration for the simulations.

Hydrocarbon/reaction	htr	prot	(exo)-prsc	endo-prsc	PCP-isom	Endo-β	(exo)-β	(de)Alkyl	Cycl	Disp
Alkanes	77	–	3604	–	74	–	2445	41	–	–
Alkenes	77	77	–	–	74	–	2455	41	13	–
(poly)Cycloalkanes	126	–	6409	152	–	150	5884	–	–	–
(poly)Cycloalkenes		126	–	–	–	150	5884	–	–	–
Cycloalkadienes	12	12	–	–	–	–	–	–	–	–
(poly)Aromatics	108	–	6052	–	–	–	4938	543	12	128
(poly)Aromatic alkenes	–	108	–	–	–	–	4936	543	12	–
Cycloalkane-(poly)aromatics	6	–	33	16	–	–	–	13	–	–
(cyclo)Alkene-(poly)aromatics	6	6	–	–	–	–	–	–	–	–

hydrocarbons accounted for in the simulations. The total number of "cracking" reactions amounts to 45,343.

The conversion of the various hydrocarbon types contained in the feed occurs in the following way. After undergoing hydride transfer, isoalkanes can be directly converted via β-scission to lighter alkenes/alkanes; while n-alkanes first have to undergo a PCP-branching reaction before the chain cleavage can occur. Aromatics dealkylate to produce benzene and (iso)alkenes/(iso)alkanes or can undergo β-scission on the side chain(s) to yield smaller aromatics and acyclic products. Cycloalkanes can be transformed through exocyclic-β-scission to smaller cycloalkanes and acyclic products or to isoalkanes/isoalkenes through endo-cyclic-β-scission (ring opening). Protolytic scission can occur on (iso)alkanes to produce smaller alkenes/alkanes, and on the side chain of cycloalkanes and aromatics to yield alkenes/alkanes and the corresponding lighter cycloalkanes and aromatics. Besides the reaction pathways involving chain cleavage, other reactions such as isomerization, alkylation, (de)protonation, hydride transfer, cyclisations, etc., also take place. In addition to the so-called "cracking reactions", 118 alkylations are involved in coke formation.

Fig. 3 shows a general representation of the different cracking and coking pathways in terms of the cracked products typically used in a refinery during the conversion of the feed. Cracked hydrocarbon products have been grouped according to their boiling point and/or carbon number in the following cuts, viz., dry gas: C_1–C_2, LPG: C_3–C_4, gasoline: C_5–C_{12}, light cyclic oil (LCO): C_{13}–C_{20} and heavy cyclic oil (HCO): C_{21+}. Coke deposited on the catalyst closes the mass balance between these product fractions and the feed. The simulation results presented in this work are expressed in terms of the yield of these hydrocarbons cuts. Based on this classification, the feed is composed by 22 wt% of LCO and 78% of HCO, vide Fig. 1.

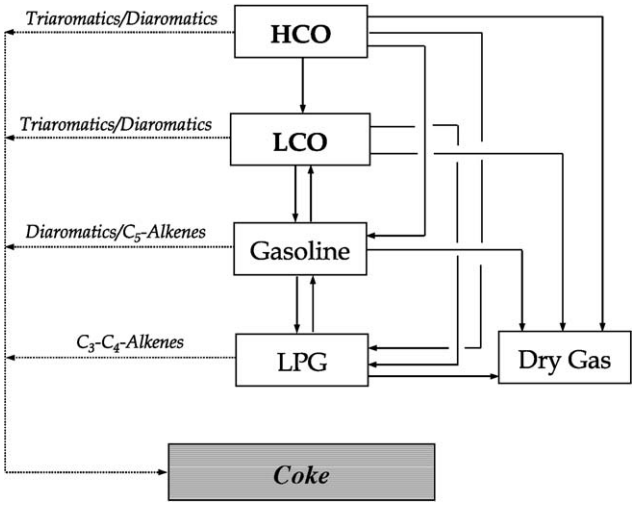

Fig. 3. Reaction routes for producing the various cracking products including coke, in terms of the cuts typically utilized in a refinery. Coking pathways are denoted with dashed arrows and hydrocarbon types that are involved in coking from the different cuts are outlined in italics.

The hydrocarbons contained in the HCO fraction crack via β-scission, protolytic scission and dealkylation to hydrocarbons in the LCO, gasoline and LPG fractions. Dry gas formation from HCO, as from any other fraction, can only occur via protolytic scission. In a similar way, hydrocarbons contained in LCO can crack to hydrocarbons in gasoline, LPG and dry gas. Hydrocarbons in the gasoline fraction are susceptible of a secondary cracking to LPG and dry gas, whereas that a minor amount of dry gas can be also produced out of LPG.

Concerning coke formation, it is illustrated in Fig. 3 that the aromatics contained in HCO and LCO fractions as well as in the gasoline fraction contribute to coke, while in the lighter fractions, i.e., LPG and C_5, are alkenes that also contribute to coke. Higher alkenes are not considered to participate directly in coking as they are susceptible to fast β-scission reactions and, hence, will occur only in small concentrations.

3.3. Kinetic parameters and deactivation functions

The fundamental character of SEMK results in rate coefficients that are independent of the feed composition. As a result, they can be estimated through the cracking of relatively simple and representative model molecules. Single-event kinetic parameters have been obtained from cracking (cyclo)alkanes/1-octene mixtures on a RE-USY equilibrium catalyst at temperatures relevant for industrial practice [30,31] in the presence of coke formation. Activation energies have been estimated via non-isothermal regression while preexponential factors have been calculated using transition state theory and statistical thermodynamic concepts [32,33]. Tables 3 and 4 display the values of a corresponding calculated set of single-event rate coefficients at 753 K for reaction families involved in the cracking of acyclic and cyclic components respectively. For the reaction of aromatics, i.e., (de)protonation, hydride transfer, protolytic scission, β-scission, etc., the obtained rate coefficients for acyclics have been used assuming that the corresponding side chains behave as a linear hydrocarbons.

The calculation of the coking rates only requires two additional rate coefficients, i.e., one for nucleus alkylation of (poly)aromatics and one for the side alkylation of (poly)aromatics [30]. Using previously determined activation energies and a common pre-exponential factor [30] results in values for the rate coefficients of 1.5×10^{-1} kg(kPa kg_{cat} s)$^{-1}$ for nucleus alkylation and 4.7×10^{-3} kg(kPa kg_{cat} s)$^{-1}$ for side chain alkylation, at 753 K.

Besides the interaction between the species in the main cracking and in the coking pathways, coke formation also affects the main cracking reaction families via active site coverage and, in a latter stage, pore blockage. The total concentration of acid sites is not adjusted to account for the deactivation by coke deposition.

Table 3
Single-event rate coefficients computed at 753 K for reactions involved in the cracking of acyclic hydrocarbons. Preexponential factors and the activation energies reported in Ref. [31] have been used.

Reaction family	Reaction type			
	p		s	t
Hydride transfer	–		8.3×10^{-8}	9.0×10^{-3}
Protonation	–		2.0×10^{-6}	4.3×10^{-5}
Deprotonation[a]	1.8×10^{7}		5.8×10^{0}	3.3×10^{-3}
Protolytic scission	1.4×10^{-8}		9.2×10^{-10}	3.2×10^{-10}
	Reaction type			
	(s,s)	(s,t)	(t,s)	(t,t)
PCP-isomerization[a]	1.3×10^{0}	3.2×10^{4}	2.3×10^{-1}	2.3×10^{-3}
β-Scission[a]	8.6×10^{-5}	2.1×10^{1}	5.8×10^{-2}	3.9×10^{-5}

[a] The units of the rate coefficients are: $\text{kmol}(\text{kg}_{\text{cat}}\,\text{s})^{-1}$ or $\text{kmol}(\text{kPa}\,\text{kg}_{\text{cat}}\,\text{s})^{-1}$.

Table 4
Single-event rate coefficients calculated at 753 K for the reactions involved in the cracking of cyclic hydrocarbons. Preexponential factors and activation energies from Ref. [31] have been used.

Reaction family	Reaction type			
	p		s	*T*
Hydride transfer	–		8.2×10^{-9}	2.6×10^{-5}
Protonation	–		2.3×10^{-7}	7.9×10^{-5}
Deprotonation[a]	–		1.1×10^{1}	3.9×10^{-2}
Exo-protolytic scission[a]	4.6×10^{-8}		2.9×10^{-8}	5.3×10^{-11}
Protonation cycloalkadienes/aromatics	–		1.1×10^{-5}	3.4×10^{-8}
Deprotonation cycloalk(adi)enes[a]	–		5.9×10^{4}	4.7×10^{-8}
Hydride transfer alkenes	–		2.1×10^{-8}	
Hydride transfer cycloalk(adi)enes	–		1.6×10^{-4}	
Disproportionation	–		1.2×10^{-1}	
	Reaction type			
	(s,s)	(s,t)	(t,s)	(t,t)
PCP-isomerization[a]	4.6×10^{2}	1.0×10^{0}	2.6×10^{-6}	3.6×10^{-3}
Endo-β-scission[a]	1.3×10^{-6}	1.4×10^{-2}	1.6×10^{-1}	5.7×10^{-4}
Exo-β-scission[a]	5.4×10^{0}	5.7×10^{4}	1.7×10^{-1}	1.6×10^{-6}

[a] The units of the rate coefficients are: $\text{kmol}(\text{kg}_{\text{cat}}\,\text{s})^{-1}$ or $\text{kmol}(\text{kPa}\,\text{kg}_{\text{cat}}\,\text{s})^{-1}$.

Instead, the decrease in available sites has been accounted for through a deactivation function, Φ, mainly because the deactivation effect is different for the various reaction families involved in catalytic cracking. The reaction rate on a catalyst with coke content C_c is calculated from the reaction rate on a fresh catalyst using Φ:

$$r_i = r_i^o \Phi \tag{22}$$

Because different reaction families require sites with a different acid strength, the deactivating effect of coke can be reaction family dependent [5,34]. An exponential dependence on the coke content is put forward:

$$\Phi_k(C_c) = \exp(-\alpha_k C_c) \tag{23}$$

In which α_k is the so-called deactivation constant. Values for α_k per reaction family were taken from Beirnaert et al. [34], cfr. Table 5. Exponentially decaying functions have been selected because of their general character in describing the loss of catalytic activity [6,35,36].

3.4. Product yields and conversion

The yields of these cuts can be easily obtained from the yields of the individual lumps as they are considered in the model and provided by the simulator. For a cut *i*, the yield is calculated by

$$x_i = \frac{G_i}{G^{\text{o}}_{\text{gas oil}}} \times 100 \tag{24}$$

The feed conversion, considering that it is composed only by LCO and HCO, is defined in terms of the mass transformed to dry gas, LPG, gasoline and coke:

$$100 - x_{\text{HCO}} - x_{\text{LCO}} \tag{25}$$

The coke yield, x_c, can be used to calculate the so-called "delta coke", a very important parameter in industrial practice that corresponds to the effective amount of coke formed per mass of catalyst after cracking, C_c, i.e., the total coke content on the catalyst after cracking minus the coke content of the regenerated catalyst, C_c^o:

$$C_c - C_c^o = x_c \frac{G^{\text{o}}_{\text{gas oil}}}{G^{\text{o}}_{\text{cat}}} = \frac{x_c}{\text{cat-to-oil ratio}} \tag{26}$$

Table 5
Deactivation constants for the various reaction types and coke formation utilized during the simulations [34].

Reaction	Value $(\text{kg}_{\text{cat}}(\text{kg}_{\text{coke}})^{-1})$
Hydride transfers	0.653
Protonations and PCP-isomerizations	0.148
Deprotonations (p) and (s)	0.031
Deprotonation (t)	0.127
β-Scissions (s,s), (s,t) and (t,s)	0.825
β-Scission (t,t)	0.407
Protolytic scission	0.445
Coking	1.951

Table 6
Riser dimensions, operating conditions and properties of the partially hydrotreated gas oil and the catalyst used in the simulations.

Parameter	Value
Dimensions	
Riser length (m)	30.0
Riser internal diameter (m)	0.94
Operating conditions	
Gas oil mass flow rate ($kg\,s^{-1}$) (MBPD)	52.6 (33.0)
Cat-to-oil ratio ($kg_{cat}(kg_{feed})^{-1}$)	6.0
Feed preheating temperature (K)	519
Temperature of the regenerated catalyst (K)	1003
Riser total pressure (kPa)	193
Catalyst properties	
Catalyst density ($kg\,m^{-3}$)	1300
Catalyst specific heat capacity ($J(kg\,K)^{-1}$)	1003
Catalyst average particle diameter (μm)	75
Feed	
Viscosity[a] ($N\,s/m^2$)	1.1×10^{-5}
Enthalpy of vaporization ($kJ(kg)^{-1}$)	150
Average molecular mass ($kg(kmol)^{-1}$)	316

[a] This is an assumed average viscosity of the main hydrocarbons in the gas phase.

4. Simulation results and discussion

The simulation and discussion of a reference case is performed first. Special attention is paid to feed conversion, cracked product distributions and temperature profiles through the riser as well as to coke formation and deactivation. Riser dimensions, operating conditions and catalyst properties used for this base case simulation are presented in Table 6. Further, an analysis of the effect of the riser dimensions, operating conditions and feed composition on the calculated cracked product distributions and temperature profiles have been performed.

4.1. Reference case

4.1.1. Gas and catalyst temperature profiles

The evolution of catalyst and gas phase temperature along the riser position at the conditions summarized in Table 6 is presented in Fig. 4. A sharp increase of the gas phase temperature at the expense of the catalyst temperature is observed during the first centimeters of the riser, which has also been observed elsewhere [7,9]. The catalyst inlet temperature is calculated as 973 K which means that a 30 K temperature decrease of the catalyst is required to fully vaporize the feed at the operating conditions used. After about 1.5 m, gas phase and catalyst temperatures reach the same value, namely 793 K. This temperature is denoted as catalyst-feed mix temperature. The rapidly achieved thermal equilibrium between the catalyst and the gas phase is attributed to the relatively large value of the corresponding heat transfer coefficient [15]. After reaching the thermal equilibrium, the temperature profile of the catalyst and gas phase hydrocarbons mixture exhibits a very slow decrease along the riser axis because of the endothermic character of cracking reactions. The temperature of solid and gas phase at the riser outlet amounts to 755 K. This is about 38 K lower than the catalyst-feed mix temperature and is in the range of typically reported differences between catalyst-feed mix and riser outlet temperatures, i.e., 30–60 K [14].

4.1.2. Cracked product distribution profiles

Fig. 5 illustrates the yield profiles of the cracked products as a function of the riser axial position obtained from simulations performed at the operating conditions displayed in Table 6. The observed profiles are in good agreement with those reported by others [7,11,13]. At the riser inlet, the fresh feed containing a significant amount of large hydrocarbons, highly susceptible for cracking, contacts the hot regenerated catalyst. This results in a vigorous cracking during the first meters of the riser yielding an important amount of lighter cracked products, in particular gasoline. Further in the riser, the cracking reactions proceed more moderately.

During the first 3 m of riser where feed conversion amounts to 47 wt%, more than 50 wt% the HCO contained in the feed has been converted while 70 wt% of the gasoline observed at the riser outlet has already been formed. The LCO yield, in particular, exhibits some remarkable behavior. An LCO decrease is observed in the first centimeters of the reactor, while in the next 2 m LCO formation from HCO is more pronounced than LCO cracking towards lighter products. The HCO conversion has become so high that LCO cracking becomes again more pronounced than LCO formation, vide Fig. 5, i.e., a positive net production rate for LCO. According to the different possibilities for the conversion of the various hydrocarbon cuts illustrated in Fig. 3, both HCO and LCO contained in the feed can directly contribute to the formation of gasoline. A detailed inspection of the gas phase composition indicates that the decrease of LCO during the first centimeters of riser is essentially caused by a very rapid consumption of mono and diaromatics which are susceptible to dealkylation, while the drastic decrease in the HCO is caused by a rapid decrease in the alkanes and mono/dicycloalkanes content.

After 10 m in the riser, about 90 wt% of the gasoline leaving the riser has already been formed, which indicates that gasoline precursors contained in the HCO and LCO fraction of the feed have

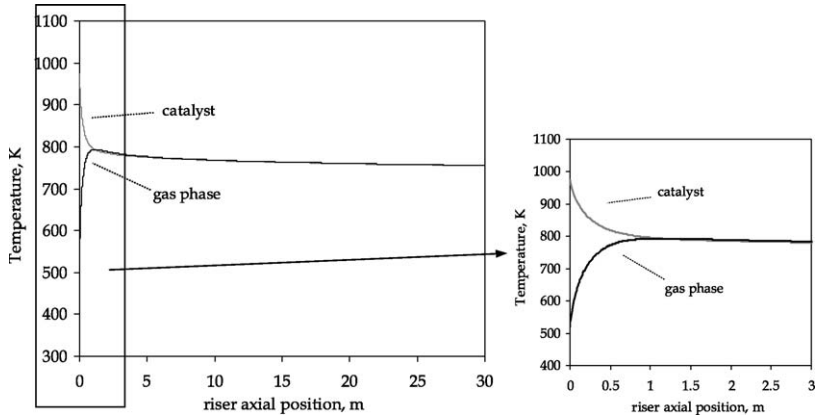

Fig. 4. Temperature of catalyst and gas products along the riser for the simulations performed over a partially hydrotreated VGO. Model equations displayed in Section 2.2, i.e., Eqs. (1), (2), (10) and (11) have been used at the operating conditions in Table 6. For the main hydrocarbons reactions, the rate coefficients used for the simulations have been computed using with preexponential factors and activation energies from Ref. [31]. For coke, kinetic data from Ref. [30].

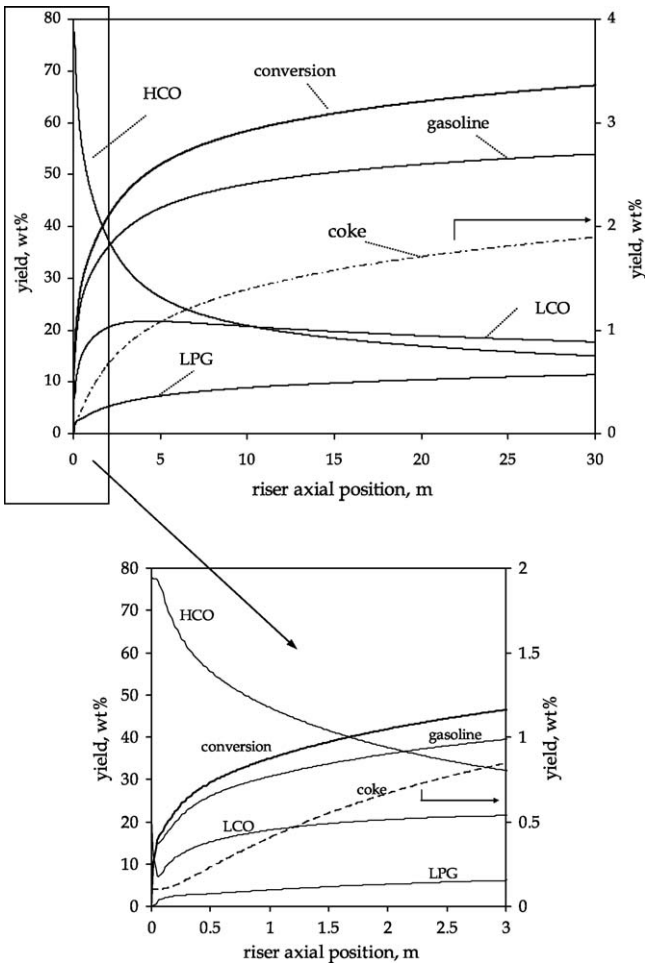

Fig. 5. Product yields and feed conversion on mass basis versus axial riser coordinate out of the catalytic cracking of a partially hydrogenated VGO. Operating conditions according to Table 6. Model equations displayed in Section 2.2, i.e., Eqs. (1), (2), (10) and (11) have been solved. For the main hydrocarbons reactions, the rate coefficients used for the simulations have been computed with the preexponential factors and activation energies from Ref. [31]. For coke, kinetic data taken from Ref. [30].

been practically converted. For the cat-to-oil ratio used in the base-case simulation, namely, 6 $kg_{cat}(kg_{feed})^{-1}$, no gasoline overcracking was detected, i.e., a decrease in the gasoline yield close to the riser outlet at relatively higher residence times. In other words, the net production rate of gasoline remains positive which is presumably associated to the nature of the feed, cfr. infra.

The simulation results allow analyzing the product yields in more detail than presented so far. Methods could be established and applied to calculate the MON and RON in gasoline. A detailed discussion is beyond the scope of this work, but as an example some features of the internal gasoline composition are highlighted. The distribution between acyclics and cyclic species was calculated at 60 wt% versus 40 wt%. The distribution of cyclic species is further split up in 29 wt% aromatics and 11 wt% saturated species, which is in agreement with generally known trends for catalytic cracking [37]. The ratio of unsaturated to saturated acyclic species was on the high side which may be related to a somewhat high value for the hydride transfer rate coefficient for acyclic species [31].

At the riser outlet the feed conversion amounts to 67 wt%, about 80 wt% of the HCO contained in the feed being converted. The gasoline and LPG yields amount to 53 wt% and 11 wt%, respectively. This feed conversion level together with the gasoline yield is in accordance with reported industrial data [38]. The residence time of the hydrocarbons in the riser was a bit lower than 2 s typical values being in the range of 2–5 s.

4.1.3. Coke formation and deactivation

The coke yield profile along the riser obtained in the reference case simulation is presented in Fig. 5. A moderate to rapid increase in coke yield is observed during the first meters of the riser, which is generally accepted for industrial operation and is typically reported in the literature [8,13]. A more pronounced increase in coke yield would have been expected when processing a feed with a higher content of (poly)aromatics, e.g., a virgin gas oil. About 60% of the coke observed at the riser outlet is formed in the first 2 m of the riser. The simulated coke yield at the riser top amounts to about 2 wt% corresponding to a coke content of 0.32 wt% at the catalyst to oil ratio investigated, cfr. Fig. 6a. Compared with typical coke yields for conventional feeds, i.e., 3–6 wt%, corresponding to coke contents from 0.6 to 1.4 wt% at a catalyst to oil ratio equal to 6.0 kg_{cat}/kg_{feed}, the presented results are somewhat lower [39]. This can be attributed to the fact that the contribution of thermal coke has not been accounted for. Moreover, a partially hydrogenated VGO with a relatively low concentration of polyaromatics as feed typically results in lower coke yields.

The reaction network leading to coke used in the SEMK is a subset of the main cracking network: intermediate species leading to coke precursors interact, i.e., compete with the species involved in the main cracking reactions. The deactivation effect of coke on the different types of elementary reaction families including coke formation is presented in Fig. 6b and c as a function of coke content. The coke formation rate is more strongly deactivated than any other elementary reaction family, which is directly related to the corresponding value of the deactivation coefficient, vide Table 5. Within the considered reaction families, the susceptibility to deactivation decreases in the following order: beta scission (s,s), (s,t) and (t,s) modes, hydride transfer and protolytic scission. Deprotonation and PCP-isomerization are deactivated to an even lesser extent. In general, at the coke levels considered in these simulations, a moderate deactivation effect is observed.

4.2. Effect of the operating and design parameters on the riser behavior

An analysis of the effect of the riser dimensions, i.e., diameter and length, as well as of some relevant variables in industrial operation, i.e., temperature of the regenerated catalyst, feed preheating temperature, catalyst to oil ratio and feed composition, on the simulation results has been performed. More attention has been paid to the effect of the operating conditions than to that of the riser dimensions because of the less pronounced impact of the latter on the feed conversion and the product distributions, vide Table 7. For instance, increasing the riser length by 5 m over the base length of 30 m and the riser diameter by 0.10 m over the base diameter of 0.94 m while maintaining the operating conditions constant, the feed conversion and product distributions are affected to a very low extent. An increase in the riser volume due to an increase of its length and/or diameter, results in a slightly higher feed conversion, gasoline and gas production.

In order to assess the effect of the operating conditions on the feed conversion and the yield of the cracked products, one parameter was varied at a time, while holding the riser dimensions and all the other parameters constant, vide Table 6. As feed composition effect, the aromatic content was modified while the fractions of the other hydrocarbons were adjusted proportionally. Moreover, the catalyst to oil ratio was varied through the catalyst flow rate. Because the axial profiles obtained were qualitatively similar to those discussed in Fig. 5, vide Section 4.1, the discussion

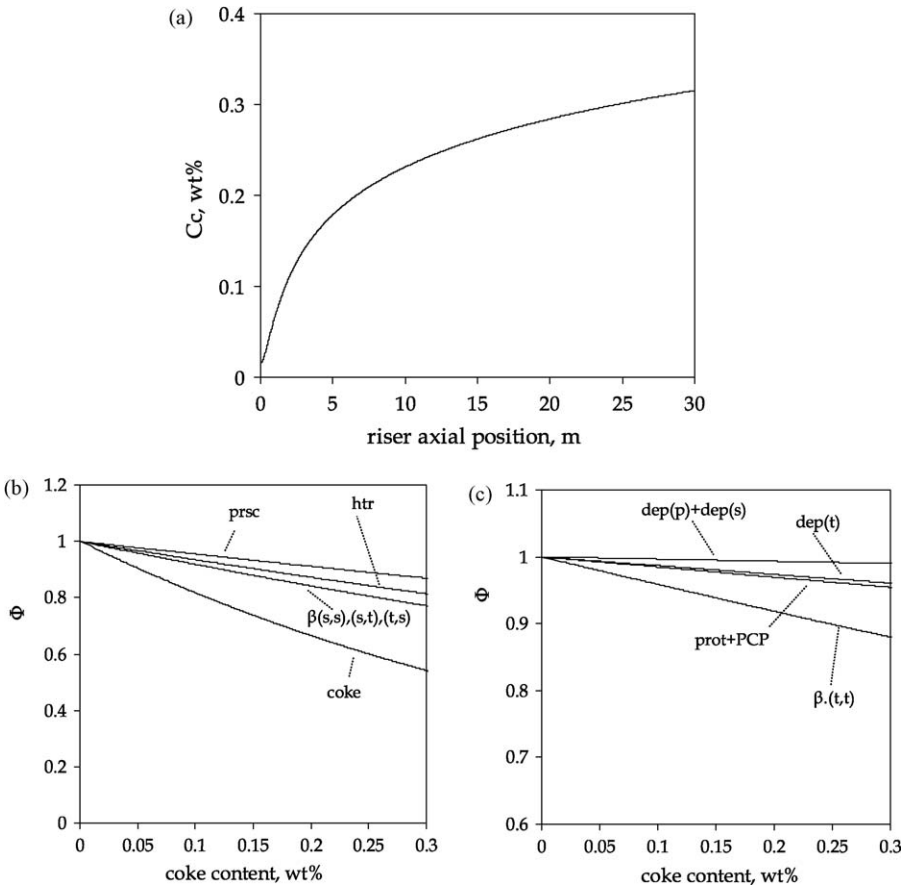

Fig. 6. (a) Coke content profile and (b) and (c) simulated deactivation functions of different elementary reaction families as a function of the catalyst coke content along the axial riser position out of the catalytic cracking of a partially hydrotreated VGO. Operating conditions according to Table 6. Model equations displayed in Section 2.2, i.e., Eqs. (1), (2), (10) and (11) have been used. For the main hydrocarbons reactions, the rate coefficients for the simulations have been computed with preexponential factors and activation energies from Ref. [31]. For coke, kinetic data taken from Ref. [30]. Deactivation constants according to Table 5, with p, s and t as primary, secondary and tertiary carbenium ions.

in the subsequent paragraphs is limited to the values at the riser outlet which are shown in Fig. 7.

4.2.1. Temperature of the regenerated catalyst and catalyst to oil ratio

From Fig. 7a and b it can be seen that the feed conversion and the product distributions are rather sensitive to variations of the temperature of the regenerated catalyst and the catalyst to oil ratio. Over the range spanned for the temperature of the regenerated catalyst, i.e., 943–1003 K, the feed conversion more than doubles. Within the cracked products, the LPG yield is more than doubled, the yield of gasoline and coke practically doubles while the consumption of LCO and HCO increases by 16 and 70%, respectively.

Increasing the catalyst to oil ratio from 5.0 to 8.0 $kg_{cat}(kg_{feed})$ results in 79% more feed conversion, i.e., from 43 to 78%, and in 50% more LPG as well as 70 and 25% more gasoline and coke, respectively. The yields of LCO and HCO decrease by 37 and 74%.

Fig. 7a and b also shows that the increment in the feed conversion and the variation in the yield of cracked products as a function of the catalyst to oil ratio and the temperature of the regenerated catalyst is not linear. E.g., for the temperature of the

Table 7
Simulated product yields and coke content at the riser outlet as well as inlet and outlet temperature for different runs obtained varying the riser dimensions. The rate coefficients for the simulations have been computed using the preexponential factors and activation energies reported in Ref. [31] for the main hydrocarbons reactions and in Ref. [30] for coking.

	Base case cfr. Table 6	Riser dimensions	
		Diameter (with respect to base diameter)	Length (with respect to a base length)
	–	+0.10 m	+5 m
Feed conversion (wt%)	67.3	69.0	68.4
Yields (wt%)			
Dry gas + LPG	11.4	11.9	11.8
Gasoline	54.0	55.1	54.7
LCO	17.7	17.0	17.2
HCO	15.0	14.0	14.3
Coke	1.9	2.0	2.0
C_c $(kg_{coke}(kg_{cat})^{-1})$	0.31	0.33	0.33
$T_{cat,inlet}$ (K)	973.2	973.2	973.2
$T_{gas/cat}$ outlet (K)	754.9	752.2	753.0

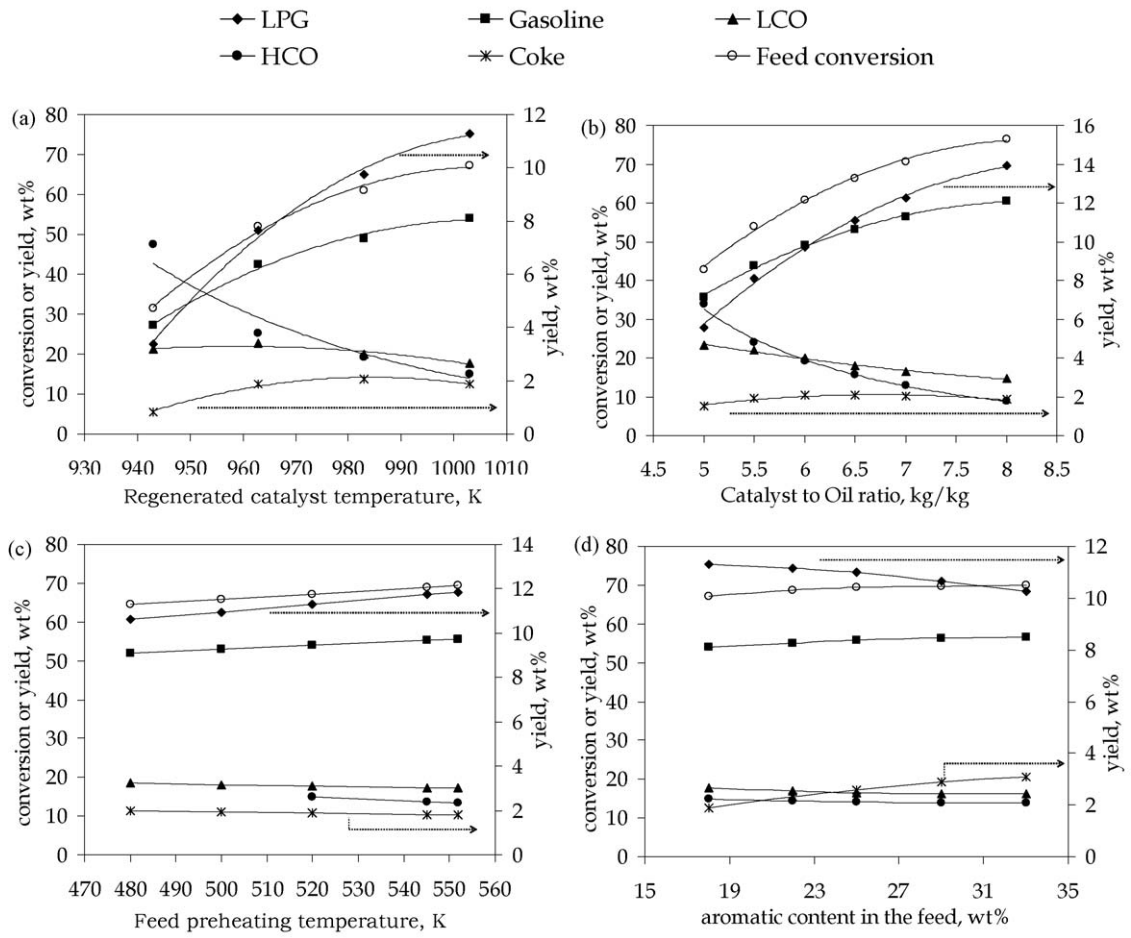

Fig. 7. Product yields and feed conversion on mass basis measured at the riser outlet when varying: (a) temperature of the regenerated catalyst, (b) catalyst to oil ratio (c) feed preheating temperature, and (d) the total aromatics content in the feed. The operating conditions different to the studied variable together with the riser dimensions displayed in Table 6 were kept constant in the simulations. An exception was the temperature of the regenerated catalyst for which 983 K was used instead of 1003 K when studying the catalyst to oil ratio effect. Solid lines have been drawn to visualize the trends.

regenerated catalyst which was incremented in regular steps of 20 K, it is clear that in the first step a pronounced increase in feed conversion and the yield of cracked products, in particular gases, is observed. More precisely, the yields of LPG and coke at 963 K are more than the double than those observed at 943 K, whereas that of gasoline and feed conversion increases by more than 50%. A further increment in the temperature of the regenerated catalyst is still reflected in higher yields of LPG and gasoline but is much less pronounced for coke. By increasing the temperature of the regenerated catalyst or the catalyst to oil ratio while keeping the feed flow rate and the feed preheating temperature constant, the catalyst inlet temperature increases. Hence, cracking reactions start at a higher temperature resulting in higher feed conversions to cracked products. In the investigated range of regenerated catalyst temperatures, i.e., from 943 to 1003 K, overcracking is only observed for the LCO fraction. That no overcracking is simulated for the gasoline fraction can be attributed to the nature of the feed. A hydrotreated gas oil typically contains a higher proportion of non-aromatic hydrocarbons, i.e., (cyclo)alkanes, which according to their chemical structure are gasoline precursors. Accordingly, the full consumption of the gasoline precursors in this feed requires of a higher reaction severity, i.e., reaction temperature and/or catalyst to oil ratio compared to other feeds, such as virgin gas oils.

4.2.2. Feed preheating temperature and feed composition

In contrast to what has been observed for the temperature of the regenerated catalyst and the catalyst to oil ratio, Fig. 7c and d shows that, in general, the feed conversion and the cracked product distributions exhibit only minor changes when varying the feed preheating temperature and the total aromatics content in the feed. Although hardly visible from Fig. 7d because of the relatively low coke yields, the latter increases linearly with amount of aromatics in the feed which is directly related to their role in coke formation.

Preheating the feed to a higher temperature in our simulations, i.e., from 480 to 552 K, only results in an increase of the feed conversion by 5% and is essentially reflected in the LPG yield, 1.2% yield increase, and the gasoline yield, 3.8% increase at the expense of HCO, while coke is practically unaffected. Higher feed preheating temperatures lead to greater catalyst-feed mix temperatures and, hence, result in higher reaction rates and feed conversion. Because of the lower heat capacity of the reacting gases compared with that of the catalyst, the effect of an increment in the feed preheating temperature is less pronounced than that of the regenerated catalyst temperature.

On the other hand, when increasing the concentration of aromatics in the feed from 18 to 33 wt%, 60% more coke is formed, whereas feed conversion and gasoline yield are only slightly affected, i.e., enhanced. The higher coke level observed when increasing the aromatics content in the feed is caused by a higher partial pressure of di and triaromatics in the gas phase, which as pointed out in previous sections, are the coke precursors contained in the HCO and LCO fractions.

5. Conclusions

A relumped Single-Event MicroKinetic model implemented in a one-dimensional riser reactor model that is pseudo-homogeneous for concentrations and heterogeneous for temperature allows to reproduce literature reported industrial reactor behavior. Product distributions and feed conversion along the riser axial coordinate in terms of typical refinery products, i.e., LPG, gasoline, LCO and coke, are in a good agreement with what is commonly encountered in the literature. Aside, the corresponding yields at the riser outlet are in line with values from the industrial practice. The same holds for the gas and solid temperature with respect to the riser position. During the first 10% of the riser length, where cracking reactions are very vigorous, about 70% of the cracked products distribution and feed conversion is determined

Considering that coke is formed through alkylation of di and triaromatics formed during cracking and of those contained in the feed with alkenes contained in the LPG and gasoline leads to satisfactory coke profiles. The coke yield at the riser outlet amounts to 2 wt% which is not far from values reported for hydrotreated feeds. By using deactivation functions, it is possible to determine the deactivation extent of the various reaction families as the cracking reaction proceeds along the riser.

A simulation model as the one developed in this work is of strategic importance to explore the effect of operating and reactor design parameters on the feed conversion, product distributions and coke deposition. The feed conversion significantly increases with the regenerated catalyst temperature and the catalyst to oil ratio, leading to enhanced gasoline and LPG production. The effect of the feed preheating temperature and aromatics content in the feed is less pronounced. Using the model, the regenerated catalyst temperature and the catalyst to oil ratio are identified as the key operating conditions for optimizing the industrial reactor behavior.

Acknowledgements

R. Quintana-Solórzano acknowledges Mexican Petroleum Institute for his PhD grant. The authors thank P. Beyney (TOTAL) for stimulating discussions. Part of this research was carried out within the framework of the Interuniversity Attraction Poles Programme funded by the Belgian Science Policy.

References

[1] A.A. Avidan, M. Edwards, Fluid Catalytic Cracking: Past and Future Challenges, vol. 6, Mobil Research and Development Corporation, 1990.
[2] R.H. Harding, A.W. Peters, J.R.D. Nee, Appl. Catal. A: Gen. 221 (2001) 389.
[3] M. Hurley, 5th FCC Forum, Organized by Stone & Webster, May, Baton Rouge, Louisiana, USA, 2002.
[4] M. Guisnet, P. Magnoux, Appl. Catal. A: Gen. 212 (2001) 83.
[5] R. Quintana-Solórzano, J.W. Thybaut, G.B. Marin, R. Lødeng, A. Holmen, Catal. Today 107–108 (2005) 619.
[6] G.F. Froment, in: C.H. Bartholomew, G.A. Fuentes (Eds.), Catalyst Deactivation, vol. 53, Elsevier Science, Amsterdam, 1997, p. 53.
[7] A. Souza, J.V.C. Vargas, O.F. Von Meien, W. Martignoni, S.C. Amico, AIChE J. 52 (2006) 1895.
[8] K.N. Theologos, I.D. Nikou, A.I. Lygeros, N.C. Markatos, AIChE J. 43 (1997) 486.
[9] A.K. Das, E. Baudrez, G.B. Marin, G.J. Heynderickx, Ind. Eng. Chem. Res. 42 (2003) 2602.
[10] C. Araujo, F. López, Ind. Eng. Chem. Eng. 45 (2006) 120.
[11] I.S. Han, J.B. Riggs, C.B. Chung, Chem. Eng. Proc. 43 (2004) 1063.
[12] S. Kumar, A. Chadha, R. Gupta, R. Sharma, Ind. Eng. Chem. Eng. 34 (1995) 3737.
[13] F. Van Landeghem, D. Nevicato, I. Pitault, M. Forissier, P. Turlier, C. Derouin, J.R. Bernard, Appl. Catal. A: Gen. 138 (1996) 381.
[14] C. Derouin, D. Nevicato, M. Forissier, G. Wild, J.-R. Bernard, Ind. Eng. Chem. Res. 36 (1997) 4504.
[15] T.A. Berry, T.R. McKeen, T.S. Pugsley, A.K. Dalai, Ind. Eng. Chem. Res. 43 (2004) 5571.
[16] M.A. Baltanás, K.K. Van Raemdonck, G.F. Froment, S.R. Mohedas, Ind. Eng. Chem. Res. 28 (1989) 899.
[17] T.M. Moustafa, G.F. Froment, Ind. Eng. Chem. Res. 42 (2003) 14.
[18] N.V. Dewachtere, F. Santaella, G.F. Froment, Chem. Eng. Sci. 54 (1999) 3653.
[19] X. Dupain, M. Makee, J.A. Moulijn, Appl. Catal. A: Gen. 297 (2006) 198.
[20] L. Hillewaert, De thermische kraking van gasoliën, experimentale studie en modellering, PhD thesis, Ghent University, 1986.
[21] D. Hudebine, J.J. Verstraete, Chem. Eng. Sci. 59 (2004) 4755.
[22] I.-S. Han, C.B. Chung, Chem. Eng. Sci. 56 (2001) 1973.
[23] V.K. Pareek, A.A. Adesina, A. Srivastava, R. Sharma, Chem. Eng. J. 92 (2003) 101.
[24] S.W. Benson, R.R. Cruickshank, D.M. Golden, G.R. Haugen, H.E. O'Neal, A.S. Rogers, R. Shaw, R. Walsh, Chem. Rev. 69 (1969) 279.
[25] A. Gupta, D.S. Rao, Chem. Eng. Sci. 56 (2001) 4489.
[26] A. Pekediz, D. Kraemer, A. Balsetti, H.I. de Lasa, Ind. Eng. Chem. Res. 36 (1997) 4516.
[27] L.R. Petzold, C. Hindmarsh, LSODA Solver for ODE Equations, 1997, Http://www.netlib.com.
[28] E. Vynckier, G.F. Froment, in: G. Astaritra, S.I. Sandler (Eds.), Kinetic and Thermodynamic Lumping of Multicomponent Mixtures, vol. 10, Elsevier Science, Amsterdam, 1991, p. 131.
[29] G.G. Martens, G.B. Marin, AIChE J. 47 (2001) 1607.
[30] R. Quintana-Solórzano, J.W. Thybaut, P. Galtier, G.B. Marin, Catal. Today 127 (2007) 17.
[31] R. Quintana-Solórzano, J.W. Thybaut, G.B. Marin, Chem. Eng. Sci. 62 (2007) 5033.
[32] J.A. Dumesic, F.D. Rudd, L.M. Aparicio, J.E. Rekoske, A.A. Treviño, The Microkinetics of Heterogeneous Catalysis, ACS Professional Reference Book, Washington, DC, 1993.
[33] G. Martens, G.B. Marin, J.A. Martens, P. Jacobs, G.V. Baron, J. Catal. 195 (2000) 253.
[34] H.C. Beirnaert, J.R. Alleman, G.B. Marin, Ind. Eng. Chem. Res. 40 (2001) 1337.
[35] G.B. Marin, G.F. Froment, Chem. Eng. Sci. 37 (1982) 759.
[36] G. Jiménez-García, R. Aguilar-López, E. León-Becerril, R. Maya-Yescas, Ind. Eng. Chem. Res. 48 (3) (2009) 1220.
[37] R. Quintana-Solórzano, J.S. Valente, F.J. Hernández-Beltrán, C.O. Castillo-Araiza, Appl. Catal. B: Environ. 81 (2008) 1.
[38] R. Sadeghbeigi, Fluid Catalytic Cracking Handbook, 2nd edition, Gulf Professional Publishing, USA, 2000.
[39] M.V. Cristea, S.P. Agachi, V. Marinoiu, Chem. Eng. Proc. 42 (2003) 67.